arXiv:1210.6081v1 [cond-mat.dis-nn] 22 Oct 2012

Strong magnetoresistance of disordered graphene

P. S. Alekseev[1], A. P. Dmitriev[1], I. V. Gornyi[1,2], and V. Yu. Kachorovskii[1]
[1] *A .F. Ioffe Physico-Technical Institute, 194021 St. Petersburg, Russia*
[2] *Institut für Nanotechnologie, Karlsruhe Institute of Technology, 76021 Karlsruhe, Germany*

(Dated: October 24, 2012)

We study theoretically magnetoresistance of graphene with the short-range disorder. The key parameter determining magnetotransport properties - the product of the cyclotron frequency and transport scattering time, depends in graphene not only on magnetic field H but also on electron energy $\varepsilon : \omega_c\tau_q \propto H/\varepsilon^2$. As a result, “quantum” ($\omega_c\tau_q \gg 1$) and “classical” ($\omega_c\tau_q \ll 1$) regimes may coexist in the same sample at fixed H, giving rise to a strong magnetoresistance. We calculate the conductivity tensor within the self-consistent Born approximation focusing on the case of relatively high temperature, when Shubnikov de Haas oscillations are suppressed by thermal averaging. We demonstrate that both at very low and at very high magnetic field the longitudinal resistivity scales as a square root of H: $[\varrho_{xx}(H) - \varrho_{xx}(0)]/\varrho_{xx}(0) \approx C\sqrt{H}$, where C is temperature-dependent factor, different in the low- and strong-field limits. Furthermore, we predict a non monotonic dependence of the Hall coefficient both on magnetic field and on the electron concentration. Finally, we discuss the case of the charged impurity potential and also find a square-root low-field dependence of magnetoresistance near the Dirac point.

PACS numbers: 72.80.Vp, 75.47.-m, 73.43.Qt

I. INTRODUCTION

Study of magnetotransport in low dimensional systems is a powerful tool to probe the nature of disorder and extract information about localization phenomena. In particular, measurements of magnetoresistance of 2D electron gas in conventional semiconductors, like GaAs, allowed one to identify a variety of different regimes, such as Drude-Boltzmann quasiclassical transport, weak localization regime and the Quantum Hall Effect (see Refs. 1 and 2 for review).

One of the simplest theoretical approaches to the problem, so called self-consistent Born approximation (SCBA), was developed in Refs. 3–6 for two-dimensional (2D) electrons with quadratic spectrum mostly for the case of short-range disorder. SCBA approach ignores localization effects. This implies that the relevant energy scale (which is the maximum of the chemical potential μ and temperature T) is large compared to the inverse transport scattering time τ_{tr}, which coincides with the quantum scattering time τ_q for short-range disorder. The key parameter of SCBA is $\omega_c\tau_q$, where ω_c is the cyclotron frequency. For weak magnetic fields, $\omega_c\tau_q \ll 1$, calculations[6] reproduce classical Drude-Boltzmann result. In the opposite limit, $\omega_c\tau_q \gg 1$, semiclassical Drude-Boltzmann approach fails, and the conductivity is given by a sum of contributions coming from well separated Landau levels (LL).[3–6]

Low-temperature magnetotransport in graphene was studied theoretically in Refs. 7–14. In Refs. 7,8 a general expression for the SCBA conductivity tensor of graphene with short-range disorder was derived and analyzed in detail for the case of well separated Landau levels. Other types of disorder were also discussed,[9–11] including disorder potentials having special types of symmetries.[12] High-temperature magnetoresistance was calculated in Ref. 13 within semiclassical Drude-Boltzman approach. In Ref. 14, a T-dependent interaction-induced contribution to the magnetoresistance (on top of a substantial positive T-independent magnetoresistance) was observed experimentally and analyzed theoretically.

A specific property of graphene compared to conventional 2D semiconductors is the linear energy dispersion of carriers,

$$\varepsilon_{\rm k} = \pm v\hbar k, \tag{1}$$

resulting in the density of states, which increases away from the Dirac point:

$$\nu_0(\varepsilon) = \frac{N|\varepsilon|}{2\pi v^2\hbar^2}. \tag{2}$$

Here $v = 10^8$ cm/c is the Fermi velocity, ε is the energy counted from the Dirac point and $N = 2 \cdot 2 = 4$ is the spin-valley degeneracy. Corresponding wave functions are given by $\exp(i\mathbf{kr})|\chi_\varphi\rangle$, where $|\chi_\varphi\rangle$ is the spinor with the components $(e^{-i\varphi/2},\ \pm e^{i\varphi/2})/\sqrt{2}$, and φ denotes the polar vector of the momentum $\mathbf{k}$.

Important consequence of the linear dispersion of graphene is that the cyclotron frequency turns out to be energy-dependent:[15]

$$\omega_c(\varepsilon) = \frac{eH}{cm(\varepsilon)} = \frac{\hbar\Omega^2}{\varepsilon}, \qquad \text{for } \varepsilon \gg \Omega. \tag{3}$$

Here H is the magnetic field, $m(\varepsilon) = \varepsilon/v^2$ is the energy-dependent cyclotron mass,

$$\Omega = \frac{v}{l} \tag{4}$$

is proportional to the distance between lowest Landau levels [see Eq. (17) below] and $l = \sqrt{e\hbar/Hc}$ is the magnetic length. Another consequence is the energy dependence of quantum and momentum relaxation times for the short-range scattering potential. Here we by definition assume that the random potential is a short-range one if its radius R satisfy the following inequalities

$$a \ll R \ll \lambda, \tag{5}$$

where a is the lattice constant and λ is the electron wavelength (this definition is different from one chosen in Refs. 16,17). Such potential does not mix valleys and can be written as[7,16]

$$\hat{V}(\mathbf{r}) = u_0 \sum_i \delta(\mathbf{r} - \mathbf{r}_{\mathrm{i}}) \begin{pmatrix} 1 & 0 \\ 0 & 1 \end{pmatrix} , \tag{6}$$

where summation is taken over impurity positions. The correlation function of $\hat{V}(\mathbf{r})$ has the same form as for 2D electrons with the quadratic spectrum: $\langle V(\mathbf{r})V(\mathbf{r}')\rangle = \kappa\delta(\mathbf{r} - \mathbf{r}')$. Here $\kappa = n_i u_0^2$ and n_i is the impurity concentration. Calculating by golden rule the quantum and transport scattering times we find that they are different and both energy-dependent:[7,15]

$$\tau_q(\varepsilon) = \frac{\gamma\hbar}{|\varepsilon|}\,, \quad \tau_{tr}(\varepsilon) = 2\tau_q(\varepsilon)\,, \tag{7}$$

where $\gamma = 2\hbar^2 v^2/\kappa$. The difference between τ_{tr} and τ_q is due to weak anisotropy of the scattering arising from spinor nature of the wave functions. Indeed, the squared scattering matrix element, $|U_{\mathbf{k}'\mathbf{k}}|^2$ is proportional to $|\langle\chi_{\varphi'}|\chi_{\varphi}\rangle|^2$ and, therefore, depends on the scattering angle $\varphi - \varphi'$. Below we assume that $\gamma \gg 1$ and , consequently, $\varepsilon\tau_q(\varepsilon)/\hbar \gg 1$. The letter inequality allows us to neglect localization effects. We also assume that disorder does not affect density of states. This condition is also satisfied provided that γ is large, with an exception for exponentially small energies,[17] $\varepsilon \sim \Delta\, e^{-\pi\gamma/2}$ (Δ is the bandwidth), which are irrelevant for this paper. Under such assumptions the conductivity in zero magnetic field is given by the Drude formula:

$$\sigma_{xx}^D = \frac{2e^2\gamma}{\pi\hbar}, \text{ for } H = 0. \tag{8}$$

We see that both ω_c and τ_q are energy-dependent and, therefore, the parameter

$$x = \omega_c \tau_q = \frac{\varepsilon_*^2}{\varepsilon^2} \tag{9}$$

can be small or large at the same sample for different ε. Here we used Eqs. (3) and (7) and introduced the energy

$$\varepsilon_* = \hbar\Omega\sqrt{\gamma} \gg \hbar\Omega, \tag{10}$$

which scales as a square root of the magnetic field:

$$\varepsilon_* \propto \sqrt{H}. \tag{11}$$

As seen from Eq. (9), at sufficiently high T the temperature window might include both the "quantum" ($x > 1$) and the "classical" ($x < 1$) regions, so that the total conductivity might show some peculiarities specific both for quantum and classical transport.

In this paper we calculate magnetoresistance (MR) of graphene with short-range disorder assuming that $\max(T, \mu) \gg \hbar\Omega$ and, consequently, the number of filled LLs is large.

The most interesting finding is related to the case $\varepsilon_* \to 0$ ($H \to 0$). We demonstrate that the dominant contribution to the low-field resistivity comes from the energy scale ε_*, which is deep below $\max(\mathrm{T}, \mu)$ in this case. This contribution is calculated within SCBA based on the approach of Ref. 7. Assuming that temperature is not too small

$$\hbar\omega_c(\varepsilon^*) \ll T \tag{12}$$

(this condition ensures that Shubnikov de Haas oscillations are suppressed by energy averaging within the temperature window) we find that for low fields ($\varepsilon_* \ll T$) the relative longitudinal resistivity scales as a square root of H:

$$\frac{\Delta\varrho_{xx}}{\varrho_{xx}(0)} \approx \frac{0.784\ \varepsilon_*}{T\cosh^2(\mu/2T)} \propto \sqrt{H}. \tag{13}$$

Here $\Delta\varrho_{xx} = \varrho_{xx}(H) - \varrho_{xx}(0)$, and $\varrho_{xx}(0) = \pi\hbar/2e^2\gamma$. For $T \ll \mu$, MR is exponentially small because the energy scale $\varepsilon \sim \varepsilon^*$ is well beyond the temperature window. However, for $T \gtrsim \mu$, low-field MR is quite large and increases with decreasing the temperature. From the side of the lowest fields, the square root dependence (13) is limited by exponentially small fields corresponding to $\varepsilon_* \sim \varepsilon_*^{min} \approx \Delta e^{-\pi\gamma/2}$. Calculation of MR at $\varepsilon_* \ll \varepsilon_*^{min}$ is not controlled because at such energies γ is renormalized to unity,[17] so that impurity potential becomes effectively strong and SCBA fails. One may expect that for $\varepsilon_* \ll \varepsilon_*^{min}$ MR becomes parabolic which implies that one should replace factor ε_*/T with $(\varepsilon_*/T)(\varepsilon_*/\varepsilon_*^{min})^3$ in Eq. (13).

We show that the square-root dependence of MR is also obtained in the opposite limit of large field, $\varepsilon_* \to \infty$ ($H \to \infty$):

$$\frac{\Delta\varrho_{xx}}{\varrho_{xx}(0)} \approx \begin{cases} 0.96\ \varepsilon_* T/\mu^2, \text{ for } T \gg \mu, \text{ and } \varepsilon_* \gg T^2/\mu, \\ 0.68\ \varepsilon_*/\mu, \text{ for } \mu \gg T, \text{ and } \varepsilon_* \gg \mu. \end{cases} \tag{14}$$

Further, we discuss the behavior of the Hall coefficient R as a function of the magnetic field and the electron concentration and demonstrate that it is a non-monotonic function of both variables.

In Fig. 1 we plotted schematically the dependence of the longitudinal resistivity and the Hall coefficient on the magnetic field for $\mu \ll T$. Importantly, square-root MR is predicted both for very law and very high fields. More detailed pictures are presented below in Figs. 4, 5, and 6. It turns out more convenient to plot all dependencies not as functions of H but as function of $\varepsilon_* \propto \sqrt{H}$. This

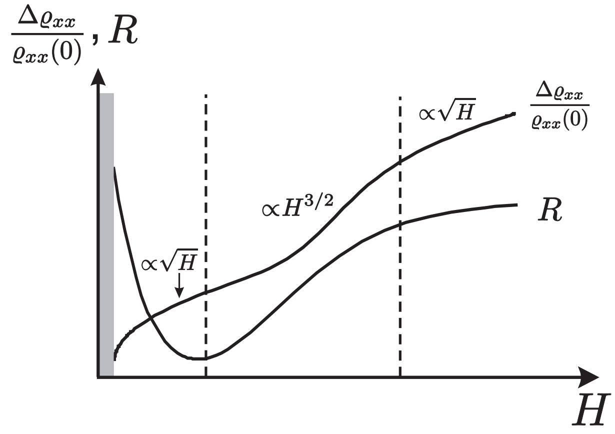

Figure 1: Schematic plot of the dependence of the longitudinal resistivity and the Hall coefficient on the magnetic field for $\mu \ll T$. Region of exponentially weak fields corresponding to $\varepsilon_* < \varepsilon_{min}$ is marked by grey color. Our theory is applicable for higher fields. Vertical dashed lines correspond to $\varepsilon_* \sim T$ and $\varepsilon_* \sim T^2/\mu$.

allows us to present the results for $\mu \ll T$ and $\mu \gg T$ in a similar way.

Finally, we analyze the case of charged impurities and show that at the Dirac point the low-field MR also scales as $\sqrt{H}$ provided that static screening of such impurities is taken into account.

II. BASIC EQUATIONS

A. Qualitative analysis

In the beginning of this section, before turning to the rigorous calculations, it is instructive to make some qualitative estimates clarifying the physics of the predicted square-root MR. To this end we note that behavior similar to given by Eq. (13) may be obtained already within classical Drude-Boltzmann. Indeed, this approach yields

$$\sigma_{xx}^{D}(\varepsilon) = \frac{2e^2\gamma}{\pi\hbar}\frac{1}{1+[\omega_c(\varepsilon)\tau_{tr}(\varepsilon)]^2} \tag{15}$$

$$= \frac{2e^2\gamma}{\pi\hbar}\left(1-\frac{4\varepsilon_*^4}{\varepsilon^4+4\varepsilon_*^2}\right), \tag{16}$$

where we used Eq. (9). Importantly, the second term in the r.h.s. of Eq. (16) is peaked near $\varepsilon = 0$ within the width on the order of ε_*. Consider for simplicity the case $\mu = 0$ assuming that $\varepsilon_* \ll T$. Averaging of Eq. (16) over energy within the temperature window yields two terms: field independent contribution $2e^2\gamma/\pi\hbar$ and the contribution of the peak which is on the order of $-(2e^2\gamma/\pi\hbar)(\varepsilon_*/T)$. Taking into account that at low fields transverse conductivity is small and, consequently, $\varrho_{xx} \approx 1/\sigma_{xx}$, we find $\Delta\varrho_{xx}/\varrho_{xx}(0) \sim \varepsilon_*/T \propto \sqrt{H}$. It turns out, however, that such an analysis yields incorrect value of the numerical coefficient in the low-field asymptotic of MR [see discussion after Eq. (53)]. Indeed, purely classical Drude-Boltzmann approach is valid for $\varepsilon \gg \varepsilon_*$ and fails at relevant energies $\varepsilon \sim \varepsilon_*$ where Landau levels start to separate. On the other hand, for $\varepsilon \ll \varepsilon_*$ Landau levels are well separated and the longitudinal conductivity contains the density of states squared. This after thermal averaging also leads to a $\sqrt{H}-$contribution to MR which comes from separated Landau levels (see, e.g., Refs. 18 and 21) and has essentially quantum nature (despite temperature is higher than inter-level distance). In the calculations below we use a rigorous approach based on SCBA, which treats both, classical and quantum, mechanisms of the square-root-magnetoresistance on equal footing and allows one to describe crossover between classical and quantum regions at $\varepsilon \sim \varepsilon_*$.

B. Self-consistent Born Approximation for graphene with short-range disorder

Inequality (5) ensures that disorder does not mix valleys K and K′, so that one may calculate the conductivity in one valley and then simply multiply the obtained result by the factor 2. The single-valley Hamiltonian of an electron in graphene in the perpendicular magnetic field reads:[15,16]

$$\hat{H} = \hat{H}_0 + V_{\rm imp}(\mathbf{r})\,,$$

$$\hat{H}_0 = v\,\hbar\left(\hat{\boldsymbol{\sigma}}\cdot\left[\hat{\mathbf{k}}+\frac{e}{c\hbar}\mathbf{A}(\mathbf{r})\right]\right)\,,$$

where e is the absolute value of electron charge, $V_{\rm imp}(\mathbf{r})$ is the random impurity potential. The eigenenergies and eigenfunctions of H_0 are given by

$$\varepsilon_n = \hbar\Omega\ \mathrm{sign}(n)\sqrt{2|n|},\ \ \psi_{n,k}(x,y) = e^{-iky}\chi_n(x-kl^2), \tag{17}$$

where Ω is given by Eq. (4) and

$$\chi_n(x) = \begin{cases} \dfrac{1}{\sqrt{2}}\begin{bmatrix} h_{|n|-1}(x) \\ \mathrm{sign}(n)\ h_{|n|}(x)\end{bmatrix}, & \text{for } n = \pm1,\pm2,\ldots; \\[2ex] \begin{bmatrix} 0 \\ h_0(x)\end{bmatrix}, & \text{for } n = 0. \end{cases} \tag{18}$$

Here $h_n(x)$ are the normalized wave functions of the harmonic oscillator with the frequency Ω and mass $\hbar/sl$. As seen from Eq. (17), the energy-dependent cyclotron frequency is connected with Ω by Eq. (3) while the relevant energy scale ε_* is given by Eq. (10) and corresponds to high LL, so that we can use the SCBA for calculation of the resistivity.

In the SCBA, the electron Green function in the short-range potential is given by[7]

$$\hat{G}(\varepsilon) = \frac{1}{\varepsilon - \hat{H}_0 - \hat{\Sigma}}, \tag{19}$$

where self-energy is found from the following equation

$$\hat{\Sigma} = \kappa \left\langle \mathbf{r} \left| \frac{1}{\varepsilon - \hat{H}_0 - \hat{\Sigma}} \right| \mathbf{r} \right\rangle . \tag{20}$$

As shown in Ref. 7, $\hat{\Sigma}$ is 2×2 matrix having nonzero matrix elements between χ_n and χ_{-n}. However, at high energies corresponding to high Landau levels, $\hat{\Sigma}$ becomes simply proportional to the unit matrix

$$\hat{\Sigma}(\varepsilon) \approx \Sigma(\varepsilon) \begin{pmatrix} 1 & 0 \\ 0 & 1 \end{pmatrix}, \text{ for } \varepsilon \gg \hbar\Omega,$$

where

$$\Sigma(\varepsilon) = \Delta(\varepsilon) \pm i\Gamma(\varepsilon) \tag{21}$$

(signs $+$ and $-$ corresponds to advanced and retarded self-energies, respectively). In this approximation, Σ obeys[7]

$$\Sigma = \frac{(\hbar\Omega)^2}{\gamma} \sum_{n=0}^{N_{max}} \frac{\varepsilon - \Sigma}{(\varepsilon - \Sigma)^2 - \varepsilon_n^2}. \tag{22}$$

Here N_{max} is the ultraviolet cutoff. The sum entering Eq. (22) can be calculated by using the identity

$$\sum_{n=0}^{N_{max}} \frac{1}{N - W} \approx \ln\left(\frac{N}{W}\right) - \pi \cot(\pi W), \tag{23}$$

valid for $N_{max} \gg \mathrm{Re}(W) \gg 1$, $\mathrm{Im}(W) \lesssim \mathrm{Re}(W)$, $\mathrm{Im}(W) > 0$. From Eqs. (22) and (23) we obtain

$$\Sigma \approx \frac{\varepsilon - \Sigma}{2\gamma} \left\{ \ln\left[\frac{2N_{max}(\hbar\Omega)^2}{(\varepsilon - \Sigma)^2}\right] - \pi \cot\left[\pi \frac{(\varepsilon - \Sigma)^2}{2(\hbar\Omega)^2}\right] \right\}. \tag{24}$$

The logarithm entering Eq. (24) is a smooth function of ε and leads to a linear in ε correction to Σ, which is irrelevant provided that $\gamma \gg \ln N_{max}$ (see also discussion of SCBA in graphene in Ref. 12). We substract this correction from Σ and for simplicity use the same notation Σ for thus redefined self-energy. Then we find from Eq. (24) the system of coupled equations for Δ and Γ :

$$\Delta = \frac{\Gamma_0 \ \sin\left[2\pi(\varepsilon - \Delta)/\hbar\omega_c\right]}{\cosh\left[2\pi\Gamma/\hbar\omega_c\right] - \cos\left[2\pi(\varepsilon - \Delta)/\hbar\omega_c\right]}, \tag{25}$$

$$\Gamma = \frac{\Gamma_0 \ \sinh\left[2\pi\Gamma/\hbar\omega_c\right]}{\cosh\left[2\pi\Gamma/\hbar\omega_c\right] - \cos\left[2\pi(\varepsilon - \Delta)/\hbar\omega_c\right]}, \tag{26}$$

where $\Gamma_0(\varepsilon) = \hbar/2\tau_q(\varepsilon)$. We also normalize Γ by its value at zero magnetic field introducing the quantity

$$z(\varepsilon) = \frac{\Gamma(\varepsilon)}{\Gamma_0(\varepsilon)} = \frac{\nu(\varepsilon)}{\nu_0(\varepsilon)}, \tag{27}$$

Here $\nu(\varepsilon)$ is the density of states in the magnetic field. The solution of Eqs. (25) and (26) can be found analytically in the limiting cases $\varepsilon \gg \varepsilon_*$ $(x \ll 1)$ and $\varepsilon \ll \varepsilon_*$ $(x \gg 1)$:

$$\Delta = \begin{cases} 2\Gamma_0 e^{-\pi/x} \sin\left(\dfrac{2\pi\varepsilon}{\hbar\omega_c}\right), \text{ for } \varepsilon \gg \varepsilon_*, \\ \displaystyle\sum_n \vartheta\left(\frac{\varepsilon - \varepsilon_n}{\Gamma_n}\right) \frac{\varepsilon}{2}, \text{ for } \varepsilon \ll \varepsilon_*. \end{cases} \tag{28}$$

$$z \approx \begin{cases} 1 + 2ae^{-\pi/x} + 2(2a^2 - 1)\left(1 - \dfrac{2\pi}{x}\right) e^{-2\pi/x}, \text{ for } \varepsilon \gg \varepsilon_*; \\ \displaystyle\sqrt{\frac{2x}{\pi}} \sum_n \vartheta\left(\frac{\varepsilon - \varepsilon_n}{\Gamma_n}\right) \sqrt{1 - \left(\frac{\varepsilon - \varepsilon_n}{\Gamma_n}\right)^2}, \text{ for } \varepsilon \ll \varepsilon_*. \end{cases} \tag{29}$$

Here

$$a = \cos\left(\frac{2\pi\varepsilon}{\hbar\omega_c}\right), \tag{30}$$

$\vartheta(y)$ is equal to unity (zero) for $|y| < 1$ $(|y| > 1)$ and

$$\Gamma_n = \Gamma(\varepsilon_n) = \hbar\sqrt{\frac{2\omega_c(\varepsilon_n)}{\pi\tau_q(\varepsilon_n)}}. \tag{31}$$

In the first line of Eq. (29) we expanded z up to the second order with respect to $\exp(-\pi/x)$. As seen from Eqs. (3),(7) and (31), Γ_n actually does not depend on n for the case of short-range disorder which we concern with: $\Gamma_n = \Gamma_\Omega = const$. Here

$$\Gamma_\Omega = \hbar\Omega\sqrt{\frac{2}{\pi\gamma}}. \tag{32}$$

Hence, the widths of different LLs are equal, but the distance $\hbar\omega_c$ between neighbor LLs decreases with increasing ε. We also see that self-energy changes periodically with ε on the scale $\hbar\omega_c$. Both the period ad the shape of these oscillations slowly depends on energy due to energy dependence of x. The density of electron states, $\nu(\varepsilon)$, following from Eqs. (27) and (29) is plotted in Fig. 2 for $\varepsilon_* \ll \max(T, \mu)$. At low energies, $x \ll 1$, LLs are well separated, while for $x \gg 1$ density of states is given by zero-field density, Eq. (2), up to exponentially small oscillating terms.

III. CALCULATION OF THE CONDUCTIVITY

The conductivity tensor is given by thermal averaging of energy-dependent tensor $\sigma_{ij}(\varepsilon)$

$$\sigma_{ij} = \int_{-\infty}^{\infty} d\varepsilon \left[-\frac{\partial n_F(\varepsilon)}{\partial\varepsilon}\right] \sigma_{ij}(\varepsilon). \tag{33}$$

The longitudinal conductivity $\sigma_{xx}(\varepsilon)$ is calculated by summation of ladder diagrams.[7] The result is given by

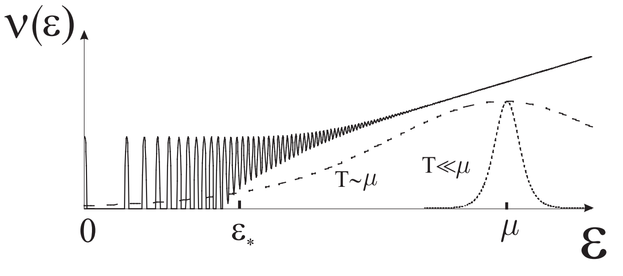

Figure 2: Density of electron states in graphene with short range disorder (solid line) and the derivative of the Fermi function for the temperatures $T \ll \mu$ and $T \sim \mu$ (dashed lines).

Eq. (4.13) of Ref. 7. Using Eq. (23) one may rewrite this result in terms of $z(\varepsilon)$

$$\sigma_{xx}(\varepsilon) = \frac{2e^2\gamma}{\pi\hbar}\frac{z(\varepsilon)^2}{z(\varepsilon)^2 + [\omega_c(\varepsilon)\tau_{tr}(\varepsilon)]^2}\,. \tag{34}$$

For high energies $x \to 0$, so that $z \to 1$ [see Eq. (29)] and we obtain Drude result, Eq. (15). For $x \gg 1$, we find from Eqs. (34) and (29) the conductivity near n-th LL[7]

$$\sigma_{xx}(\varepsilon) = \begin{cases} \dfrac{2e^2 n}{\pi^2\hbar}\left[1 - \left(\dfrac{\varepsilon-\varepsilon_n}{\Gamma_\Omega}\right)^2\right], & \text{for } |\varepsilon-\varepsilon_n| < \Gamma_\Omega, \\ 0\,, \quad \text{for } |\varepsilon-\varepsilon_n| > \Gamma_\Omega. \end{cases} \tag{35}$$

We note that Eq. (34) may be obtained from Eq. (15) by replacement of $1/\tau_{tr}(\varepsilon)$ with $z(\varepsilon)/\tau_{tr}(\varepsilon)$. Hence, the only difference of the SCBA result compared to the Drude one is the renormalization of the density of states given by Eq. (27).

The calculation of $\sigma_{xy}(\varepsilon)$ is more subtle. Simplest approximation based on summation of ladder diagrams leads to Drude-like formula with renormalized scattering time,

$$\sigma_{xy}^{I}(\varepsilon) = \frac{2e^2\gamma}{\pi\hbar}\frac{\omega_c(\varepsilon)\tau_{tr}(\varepsilon)z(\varepsilon)}{z^2(\varepsilon) + [\omega_c(\varepsilon)\tau_{tr}(\varepsilon)]^2}, \tag{36}$$

in a full analogy with Eq. (34). In fact, there also exists another contribution to transverse conductivity, which is expressed via thermodynamical properties of electron gas:[19,20]

$$\sigma_{xy}^{II}(\varepsilon) = ec[\partial n/\partial H]_\varepsilon. \tag{37}$$

Here $n = n(\varepsilon, H)$ is the electron concentration in magnetic field for zero temperature and chemical potential coinciding with ε. The derivative over H is taken for fixed ε. Hence,

$$\sigma_{xy}(\varepsilon) = \sigma_{xy}^{I}(\varepsilon) + \sigma_{xy}^{II}(\varepsilon). \tag{38}$$

In fact, $\sigma_{xy}^{II}(\varepsilon)$ yields essential contribution to $\sigma_{xy}(\varepsilon)$ for $\varepsilon \ll \varepsilon_*$ when Landau levels are well separated (in the opposite case of overlapping Landau levels $\sigma_{xy}^{II}(\varepsilon)$ is exponentially small).

Let us now do the integral in Eq. (33). As follows from Eq. (29), the dependence $\sigma_{ij}(\varepsilon)$ contains fast oscillations on the scale $\hbar\omega_c$, the shape and the period of the oscillations being energy-dependent due to energy dependence of x. Therefore, for relatively high temperature the integration in Eq. (33) may be performed in two steps. First, we average $\sigma_{ij}(\varepsilon)$ in Eq. (33) by the energy interval $\delta\varepsilon$, such that $\varepsilon \gg \delta\varepsilon \gg \hbar\omega_{\rm c}(\varepsilon)$. Such an averaging "filters" the Shubnikov oscillations and results in a smooth function $\bar\sigma_{ij}(\varepsilon)$. One can also show that after averaging $\bar\sigma_{xy}^{II}$ can be neglected[22] (provided that $\gamma \gg 1$) both for overlapping[23] ($\varepsilon \gg \varepsilon_*$) and for separated ($\varepsilon \ll \varepsilon_*$) Landau levels. Hence below we use

$$\bar\sigma_{xy}(\varepsilon) \approx \bar\sigma_{xy}^{I}(\varepsilon).$$

It is convenient to write $\bar\sigma_{ij}$ in the following form

$$\bar\sigma_{ij}(\varepsilon) = \sigma_{ij}^{\rm D}(\varepsilon)\,\eta_{ij}(\varepsilon)\,, \tag{39}$$

where $\eta_{ij}(\varepsilon)$ are dimensionless factors. From Eqs. (29), (30), (34), and (36) we find asymptotical behavior of η_{ij} :

$$\eta_{xx} \approx \begin{cases} 1 - 24x^2 e^{-2\pi/x} = 1 - \dfrac{24\varepsilon_*^4}{\varepsilon^4} e^{-2\pi\varepsilon^2/\varepsilon_*^2}, \text{ for } \varepsilon \gg \varepsilon_*, \\ C_1\sqrt{x} = C_1\varepsilon_*/\varepsilon, \text{ for } \varepsilon \ll \varepsilon_*, \end{cases} \tag{40}$$

$$\eta_{xy} \approx \begin{cases} 1 + 2e^{-2\pi/x} = 1 + 2e^{-2\pi\varepsilon^2/\varepsilon_*^2}\ , \text{ for } \varepsilon \gg \varepsilon_*, \\ 1\ , \text{ for } \varepsilon \ll \varepsilon_*. \end{cases} \tag{41}$$

Here $C_1 = 8\sqrt{2}/3\pi\sqrt{\pi} \approx 0.68$. For arbitrary values of ε the factors η_{ij} have been calculated numerically. The dependencies $\bar\sigma_{xx}(\varepsilon)$ and $\bar\sigma_{xy}(\varepsilon)$ are plotted schematically in Fig. 3. In this picture we took into account that $\sigma_{xx}(\varepsilon) = \sigma_{xx}(-\varepsilon), \sigma_{xy}(\varepsilon) = -\sigma_{xy}(-\varepsilon)$ because of the particle-hole symmetry. In the high-energy asymptotics we keep exponentially small terms [proportional to $\exp(-2\pi/x)$], since they are important in the calculation of MR in the limit of low temperature and low field (see below). It is worth also noting that averaged longitudinal conductivity is not exactly zero at $\varepsilon = 0$ but saturates at $\varepsilon \sim \hbar\Omega$ at a quite small value: $\bar\sigma_{xx}\pi\hbar/2e^2\gamma \sim 1/\sqrt{\gamma} \ll 1$.

As a second step, we calculate σ_{ij} by replacing $\sigma_{ij}(\varepsilon)$ with $\bar\sigma_{ij}(\varepsilon)$ in Eq. (33):

$$\sigma_{ij} = \int d\varepsilon \left[-\frac{\partial n_F(\varepsilon)}{\partial\varepsilon}\right]\bar\sigma_{ij}(\varepsilon), \tag{42}$$

and substitute thus obtained σ_{ij} into expression for longitudinal resistivity

$$\varrho_{xx} = \frac{\sigma_{xx}}{\sigma_{xx}^2 + \sigma_{xy}^2}. \tag{43}$$

The result of calculations depends on relation between tree relevant energies T, μ and ε_*. The magnetic field dependence of ϱ_{xx} is encoded in the square-root scaling of ε_*. Below we discuss separately the cases of low and high temperatures.

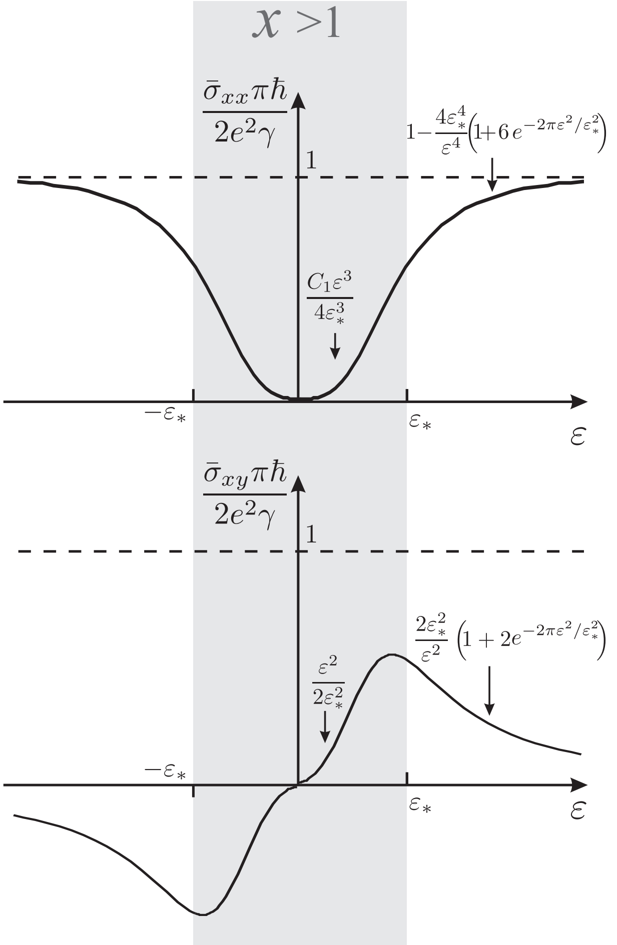

Figure 3: Dependence of $\bar{\sigma}_{xx}$ and $\bar{\sigma}_{xy}$ on energy. The region $x > 1$ is marked by grey color.

A. Low temperatures, $T \ll \mu$.

We start with discussing of high-field limit, $\varepsilon_* \gg \mu$. Since integral over energy in Eq. (42) is concentrated in the narrow temperature window near $\varepsilon = \mu$ we can use low energy-asymptotics for $\bar{\sigma}_{xx}$ and $\bar{\sigma}_{xy}$, see Fig. 3. Doing so, and replacing in Eq. (42) $[-\partial n_F(\varepsilon)/\partial\varepsilon]$ with $\delta(\varepsilon-\mu)$, we find

$$\sigma_{xx} \approx \frac{2e^2\gamma}{\pi\hbar}\frac{C_1\mu^3}{4\varepsilon_*^3}, \quad \sigma_{xy} \approx \frac{2e^2\gamma}{\pi\hbar}\frac{\mu^2}{2\varepsilon_*^2}. \tag{44}$$

We see that $\sigma_{xx} \ll \sigma_{xy}$. Therefore, $\varrho_{xx} \approx \sigma_{xx}/\sigma_{xy}^2$ and

$$\frac{\Delta\varrho_{xx}}{\varrho_{xx}(0)} \approx \frac{C_1\varepsilon_*}{\mu} \propto \sqrt{H}, \quad \text{for} \;\; \varepsilon_* \gg \mu. \tag{45}$$

Next we consider the opposite case $\varepsilon_* \ll \mu$. In this case, there are different competing contributions to magnetoresistance. First contribution is obtained quite analogously to high-field limit by replacing derivative from Fermi distribution with delta function. In this approximation, $\sigma_{xx} = \bar{\sigma}_{xx}(\mu), \sigma_{xy} = \bar{\sigma}_{xy}(\mu)$. As follows from Eqs. (40) and (41), in the limit of large μ these conductivities differ from Drude values by exponentially small terms only. It is well known that in the Drude-Boltzmann approximation MR is absent. Hence, MR should be exponentially small. Indeed, substituting $\bar{\sigma}_{xx}(\mu)$ and $\bar{\sigma}_{xy}(\mu)$ into Eq. (43), using Eqs.(39), (40), and (41), and keeping terms on the order of $\exp(-2\pi/x)$ we obtain

$$\frac{\Delta\varrho_{xx}}{\varrho_{xx}(0)} \approx \frac{8\varepsilon_*^4}{\mu^4}e^{-2\pi\mu^2/\varepsilon_*^2}, \quad \text{for} \;\; \varepsilon_* \ll \mu. \tag{46}$$

There are two other contributions which may compete with this exponentially small result. Both contributions arise due to finite value of temperature, which was in fact assumed to be zero while deriving Eq. (46). Let us now take into account that the function

$$-\frac{\partial n_F(\varepsilon)}{\partial\varepsilon} = \frac{1}{4T\cosh^2[(\varepsilon-\mu)/2T]} \tag{47}$$

is peaked near $\varepsilon = \mu$ within a finite width on the order of T. First of all, there exists a correction to magnetoresistance due to a small variation of $x(\varepsilon)$ within a temperature window. To find this correction we put $\eta_{ij} \approx 1$, expand $\bar{\sigma}_{ij}(\varepsilon)$ near $\varepsilon = \mu$ up to the second order with respect to $\varepsilon - \mu$, calculate integral Eq. (42) and use Eq. (43). As a result, we get a quadratic-in-H MR

$$\frac{\Delta\varrho_{xx}}{\rho_{xx}(0)} = \frac{C_2T^2\varepsilon_*^4}{\mu^6} \propto H^2, \tag{48}$$

where $C_2 \approx 16\pi^2/9$. This correction becomes lager than Eq. (46) for relatively weak fields such that $\varepsilon_* \ll \varepsilon_1$, where

$$\varepsilon_1 = \frac{\sqrt{2\pi}\mu}{\ln^{1/2}(8\mu^2/C_2T^2)}. \tag{49}$$

At very low magnetic fields, another contribution comes into play, namely, the contribution to integral Eq. (42) from the energies $\varepsilon \sim \varepsilon^*$ which are well beyond the temperature window. To find this contribution we first write $\bar{\sigma}_{xx}(\varepsilon)$ in the following way

$$\bar{\sigma}_{xx}(\varepsilon) = \frac{2e^2\gamma}{\pi\hbar}[1 - f(\varepsilon/\varepsilon_*)]. \tag{50}$$

The function $f(y)$ has maximum at $y = 0$ and decays when y becomes larger than 1, or, equivalently, ε becomes larger than ε_* (see Fig. 3)

$$f(y) \approx \begin{cases} \dfrac{4}{y^4}, & \text{for } y \gg 1 \ (\varepsilon \gg \varepsilon_*); \\ 1 - C_1y^3/4, & \text{for } y \ll 1 \ (\varepsilon \ll \varepsilon_*). \end{cases} \tag{51}$$

Here we neglected exponentially small corrections to f at large ε and introduced dimensionless variable $y = \varepsilon/\varepsilon_* = 1/\sqrt{x}$. Let us now assume that ε^* is smaller than T. Then one can replace $[-\partial n_F(\varepsilon)/\partial\varepsilon]$ with its value at zero energy $-n_F'(0)$, while calculating the contribution to σ_{xx} coming from the region $\varepsilon \sim \varepsilon^*$. Doing so, we obtain

$$\sigma_{xx} = \frac{2e^2\gamma}{\pi\hbar}\left[1 - 2C_3\varepsilon_*|n_F'(0)|\right], \tag{52}$$

where dimensionless constant C_3 is given by the integral

$$C_3 = \int\limits_0^\infty dy\ f(y) = 1.568. \tag{53}$$

It is instructive to compare the obtained result with the "purely classical" calculation which ignores existence of LLs. On the formal level, such an approximation implies replacement η_{ij} with unity in Eq. (42). Simple calculation (see also discussion in Sec.II A) shows that thus calculated conductivity can be presented in the same form as Eq. (52), where one should replace C_3 with

$$C_3^D = \int\limits_0^\infty dy\left(1 - \frac{1}{1+4x^2}\right) = \int\limits_0^\infty dy \frac{4}{y^4+4} = \pi/2 = 1.571. \tag{54}$$

This value is close but different from C_3, so that discreteness of LLs should be taken into account. Now we take into account that $\sigma_{xx} \gg \sigma_{xy}$, so that $\varrho_{xx} \approx 1/\sigma_{xx}$ and

$$\frac{\Delta\varrho_{xx}}{\rho_{xx}(0)} \approx 2C_3\varepsilon_*|n_F'(0)| \propto \sqrt{H}, \tag{55}$$

Since T is by assumption much smaller than μ, we conclude that MR is exponentially small:

$$\frac{\Delta\varrho_{xx}}{\rho_{xx}(0)} \approx \frac{2C_3\varepsilon_*}{T}e^{-\mu/T}. \tag{56}$$

Comparing Eq. (56) with Eq. (48) we see that the former contribution dominates when $\varepsilon_* \ll \varepsilon_2$, where

$$\varepsilon_2 \sim \frac{\mu^2}{T}e^{-\mu/3T} \ll T. \tag{57}$$

Therefore, in accordance with our assumption, $\varepsilon_* \ll T$ in the regime, when Eq. (56) dominates.

Looking now more attentively at the above derivation one concludes that Eq. (55) is valid at arbitrary relation between T and μ provided that $\varepsilon_* \to 0$ (but $\varepsilon_* > \varepsilon_*^{min}$). Hence, the low-field MR is given by

$$\frac{\Delta\varrho_{xx}}{\rho_{xx}(0)} \approx \frac{C_3\varepsilon_*}{2T\cosh^2(\mu/2T)} \propto \sqrt{H}. \tag{58}$$

B. High temperatures, $\mu \ll T$.

In this case, the low field asymptotics of MR is realized at $\varepsilon_* \ll T$ and is given by Eq. (58), where one can put $\mu = 0$

$$\frac{\Delta\varrho_{xx}}{\rho_{xx}(0)} \approx \frac{C_3\varepsilon_*}{2T} \propto \sqrt{H}/T, \text{ for } \varepsilon_* \ll T. \tag{59}$$

Hence, near the Dirac point resistivity correction scales as $\sqrt{H}$ at $H \to 0$, and increases (for fixed H) with decreasing the temperature.

Let us now consider larger fields, $\varepsilon_* \gg T$. In this case, one can use low-energy asymptotics,

$$\bar{\sigma}_{xx}(\varepsilon) \approx \frac{C_1e^2\gamma}{2\pi\hbar}\,\frac{|\varepsilon|^3}{\varepsilon_*^3},\ \bar{\sigma}_{xy}(\varepsilon) \approx \frac{e^2\gamma}{\pi\hbar}\,\frac{\varepsilon|\varepsilon|}{\varepsilon_*^2}. \tag{60}$$

Thermal averaging yields

$$\begin{aligned}
&\sigma_{xx} = \\
&\frac{e^2\gamma C_1}{8\pi\hbar}\int_0^\infty d\varepsilon\frac{\varepsilon^3}{\varepsilon_*^3T}\left[\frac{1}{\cosh^2\left(\frac{\varepsilon-\mu}{2T}\right)} + \frac{1}{\cosh^2\left(\frac{\varepsilon+\mu}{2T}\right)}\right] \\
&\approx \frac{9C_1\zeta(3)}{2\pi}\frac{e^2\gamma}{\hbar}\frac{T^3}{\varepsilon_*^3},
\end{aligned} \tag{61}$$

$$\begin{aligned}
&\sigma_{xy} = \\
&\frac{e^2\gamma}{4\pi\hbar}\int_0^\infty d\varepsilon\frac{\varepsilon^2}{\varepsilon_*^2T}\left[\frac{1}{\cosh^2\left(\frac{\varepsilon-\mu}{2T}\right)} - \frac{1}{\cosh^2\left(\frac{\varepsilon+\mu}{2T}\right)}\right] \\
&\approx \frac{4\ln 2}{\pi}\frac{e^2\gamma}{\hbar}\frac{\mu T}{\varepsilon_*^2},
\end{aligned} \tag{62}$$

where ζ is Riemann zeta function, $\zeta(3) \approx 1.2$. From Eqs. (61) and (62) we find

$$\begin{aligned}
\frac{\Delta\varrho_{xx}}{\rho_{xx}(0)} &\approx \frac{4}{9C_1\zeta(3)}\,\frac{\varepsilon_*^3}{T^3}\,\frac{1}{1+\left[\dfrac{8\ln 2}{9C_1\zeta(3)}\right]^2\dfrac{\mu^2\varepsilon_*^2}{T^4}} \\
&\approx \begin{cases} C_4\varepsilon_*^3/T^3, \text{ for } T \ll \varepsilon_* \ll T^2/\mu; \\ C_5\varepsilon_*T/\mu^2, \text{ for } T^2/\mu \ll \varepsilon_*. \end{cases}
\end{aligned} \tag{63}$$

Here $C_4 = 4/9C_1\zeta(3) \approx 0.54$, $C_5 = 9C_1\zeta(3)/16(\ln 2)^2 \approx 0.96$.

The results of calculations are summarized in the Fig. 4.

IV. HALL COEFFICIENT

Using the equations derived above one can easily calculate the transverse resistivity $\varrho_{xy} = \sigma_{xy}/(\sigma_{xx}^2 + \sigma_{xy}^2)$ and the Hall coefficient

$$R = \frac{\varrho_{xy}}{H}. \tag{64}$$

Below we discuss the dependence of R on H and on the electron concentration at zero field,

$$n = \int_{-\infty}^{\infty} n_F(\varepsilon)\nu_0(\varepsilon)d\varepsilon - \int_{-\infty}^{0}\nu_0(\varepsilon)d\varepsilon. \tag{65}$$

The second term in the r.h.s. of Eq. (65) is the concentration of background electrons which compensate the positive charge of the donors in the neutrality point. One can easily check that $n = 0$ for $\mu = 0$.

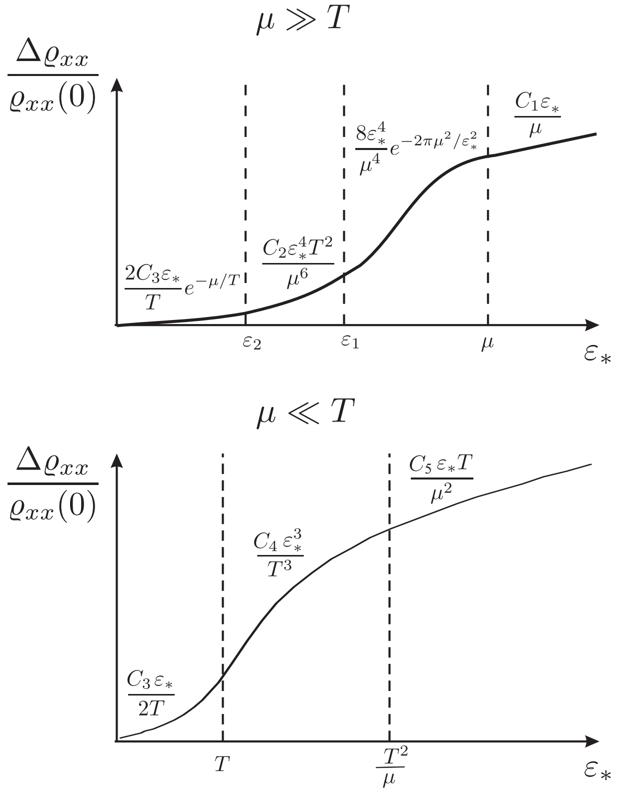

Figure 4: Resistivity of graphene for the cases $T \ll \mu$ and $T \gg \mu$ as a function of $\varepsilon_* \propto \sqrt{H}$.

For $T \ll \mu$, simple calculation yields that the Hall coefficient up to small corrections is given by conventional expression

$$R = \frac{1}{ecn}, \tag{66}$$

in the whole interval of ε_*. In this case,

$$n \approx \int_0^\mu \nu_0(\varepsilon')d\varepsilon' = \frac{N\mu|\mu|}{4\pi v^2\hbar^2}. \tag{67}$$

Consider now vicinity of the Dirac point, $\mu \ll T$. In this case,

$$n \approx \frac{N\mu T\ln 2}{\pi v^2\hbar^2}, \tag{68}$$

while the transverse conductivity is given by

$$\begin{aligned} \sigma_{xy} &= \int_0^\infty d\varepsilon \frac{\bar\sigma_{xy}(\varepsilon)}{4T}\left[\frac{1}{\cosh^2(\frac{\varepsilon-\mu}{2T})} - \frac{1}{\cosh^2(\frac{\varepsilon+\mu}{2T})}\right] \\ &\approx \frac{\mu}{2T^2}\int_0^\infty d\varepsilon\bar\sigma_{xy}(\varepsilon)\frac{\sinh(\frac{\varepsilon}{2T})}{\cosh^3(\frac{\varepsilon}{2T})}. \end{aligned} \tag{69}$$

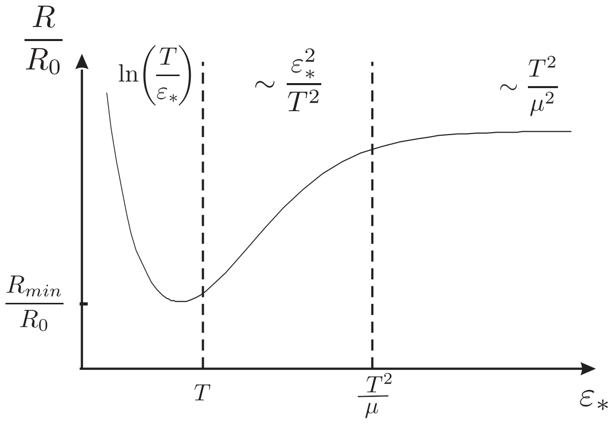

Figure 5: Dependence of the Hall coefficient, ϱ_{xy}/H, on $\varepsilon_* \propto \sqrt{H}$ at $T \gg \mu$.

For $\varepsilon_* \ll T$, the main contribution to σ_{xy} comes from the energy interval $\varepsilon_* < \varepsilon < T$, where integral in Eq. (69) is logarithmically divergent. Therefore, one may use large-ε asymptotic, $\bar\sigma_{xy} \approx (2e^2\gamma/\pi\hbar)(2\varepsilon_*^2/\varepsilon^2)$, and calculate the integral in the limits ε_* and T. Doing so we find with the logarithmic precision: $\sigma_{xy} \approx (e^2\gamma/\pi\hbar)(\mu\varepsilon_*^2/T^3)\ln(T/\varepsilon_*)$. The longitudinal conductivity is given by Eq. (52) where one can neglect small correction proportional to ε_*/T, thus writing $\sigma_{xx} \approx 2e^2\gamma/\pi\hbar$. Using these equations we find

$$R = R_0\ \ln\left(\frac{T}{\varepsilon_*}\right), \tag{70}$$

where

$$R_0 = \frac{\pi\mu v^2\hbar^2}{ecNT^3} \sim \frac{n}{n_T^2}, \tag{71}$$

where $n_T \sim NT^2/v^2\hbar^2$ is the electron concentration for $\mu \sim T$. Hence, the Hall coefficient logarithmically increases with decreasing the magnetic field. Above we noticed that our calculations are valid up to the exponentially small fields where $\varepsilon_* \sim \Delta e^{-\pi\gamma/2}$. Therefore, the maximal value of the $\ln(T/\varepsilon_*)$ is limited by $\pi\gamma/2 - \ln(\Delta/T)$.

In the opposite case, $\varepsilon_* \gg T$, the conductivity tensor is given by Eqs. (61) and (62) which yield for the Hall coefficient the following expression

$$R = R_0\frac{C_6\varepsilon_*^2/T^2}{1 + C_7\mu^2\varepsilon_*^2/T^4}, \tag{72}$$

where $C_6 = 64\ln 2/[9C_1\zeta(3)]^2 \approx 0.82$ and $C_7 = [8\ln 2/9C_1\zeta(3)]^2 \approx 0.57$. We see that the Hall coefficient linearly increases with magnetic field, $R \propto \varepsilon_*^2 \propto H$, in the interval $T \ll \varepsilon_* \ll T^2/\mu$ and saturates when ε_* becomes larger than T^2/μ. From Eqs. (71) and (72) we conclude that R is non-monotonic function of the magnetic field and has a minimum (for positive μ) at magnetic fields corresponding to $\varepsilon_* \sim T$. The minimal value of R is given by $R_{min} \sim R_0$. The dependence of R on ε_* is plotted schematically in Fig. 5.

Measurements of the Hall coefficient are usually used for extracting the density of the carriers with the help of conventional expression (66). From Eqs. (68), (70), and (72) we see that such a procedure fails near the Dirac point. Let us, therefore, discuss the dependence of R on n in details (see also Ref. 25). The analysis of above equations shows that R is a non-monotonic function of n both at low and high fields: it turns to zero for $n = 0$, has a maximum at certain $n = n_m$ and decays as $1/n$ according to Eq. (66) for $n \to \infty$ (see Fig. 6).

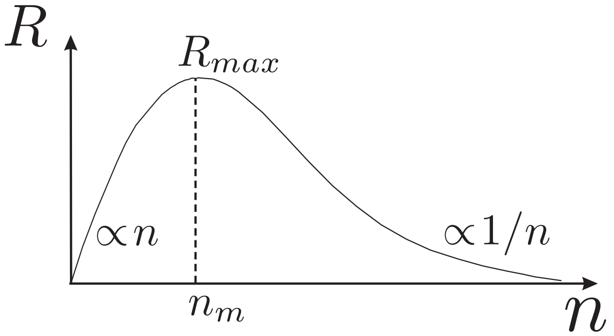

Figure 6: Dependence of the Hall coefficient on electron concentration

As follows from Eqs. (68), (70), and (71), at low fields or, equivalently, high temperatures ($\varepsilon_* \ll T$), the Hall coefficient linearly increases with n at $n \ll n_T$ ($\mu \ll T$),

$$R \sim \frac{n}{ecn_T^2} \ln(T/\varepsilon_*), \tag{73}$$

reaches the maximum value,

$$R_{max} \sim \frac{1}{ecn_T} \ln(T/\varepsilon_*), \tag{74}$$

at $n_m \sim n_T$ ($\mu \sim T$), and decays inversely proportional to the concentration at $n \to \infty$.[26]

At high field or low temperatures ($\varepsilon_* \gg T$), the dependence of R on n also has a maximum and is linear at small concentration. However, as seen from Eq. (72) there are some differences compared to low-field case. First of all, the coefficient in the linear dependence at small n turns out to be different

$$R \sim \frac{n}{ecn_T^2} \left(\frac{\varepsilon_*}{T}\right)^2. \tag{75}$$

Secondly, the maximum value of R is reached at much smaller concentration $n_m \sim (T/\varepsilon_*) n_T$ corresponding to $\mu \sim T^2/\varepsilon_* \ll T$. Equation (75) holds below this concentration while at larger n the Hall coefficient is given by conventional expression (66). The maximum Hall coefficient reads

$$R_{max} \sim \frac{1}{ecn_T} \left(\frac{\varepsilon_*}{T}\right). \tag{76}$$

V. CHARGED IMPURITIES

In the previous sections we discussed scattering by the short-range potential. One can see from above derivations, that the most interesting result, the square-root dependence of MR on H at low H is a direct consequence of the energy dependence of scattering time specific for such a scattering: $1/\tau_{tr} \propto |\varepsilon|$.

Next we discuss scattering by the charged impurities, which are often considered to give a dominant contribution to the resistivity. If we neglect screening of such impurities, we get $1/\tau_{tr} \propto |\varepsilon|^{-1}$, which implies that $\omega_c \tau_{tr}$ does not depend on energy and, consequently, the mechanism discussed above does not work. We will see, however, that the screening dramatically changes the situation and, remarkably, the low-field MR is proportional to $\sqrt{H}$, in a full analogy with short range scattering, though the temperature dependence of MR is different.

The matrix element of the scattering on a single charged impurity is given by

$$V_q = \frac{2\pi e^2/q\varkappa}{1 + (2\pi e^2/q\varkappa) N \Pi(q)}, \tag{77}$$

where $\Pi(q)$ is the static polarization operator and $\varkappa$ is the dielectric constant. Neglecting screening and using golden rule we find that transport scattering rate is inversely proportional to the energy. Let us now take screening into account. For simplicity, we will consider the low field asymptotic only focusing on the MR at the Dirac point ($\mu \ll T$).

The general expression for polarization operator at the Dirac point was derived in Ref. 24. For our purposes it is sufficient to know the asymptotical expression for $\Pi(q)$ at $q \ll T/\hbar v$:

$$\Pi(q) \approx \frac{T \ln 2}{\pi \hbar^2 v^2}, \text{ for } q \ll T/\hbar v. \tag{78}$$

Indeed, as we discussed in the previous sections the main contribution to resistivity at weak fields comes from the low energies, $\varepsilon \ll T$. Since transferred momentum $\hbar q$ is on the order of ε/v, we conclude that relevant momenta are smaller than $T/\hbar v$. Assuming also that $e^2/\hbar v \varkappa \sim 1$ we find that

$$V_q \approx \frac{1}{\Pi} \approx \frac{\pi \hbar^2 v^2}{NT \ln 2}. \tag{79}$$

We see that at low electron energies scattering matrix element does not depend on the energy just as in the case of the short range potential. Hence, in order to find low-field MR one should make the following replacement $u_0 \to u_0' = \pi \hbar^2 v^2 / NT \ln 2$ and, consequently,

$$\gamma \to \gamma' = \frac{2N^2 (\ln 2)^2 T^2}{n_i \pi^2 \hbar^2 v^2}. \tag{80}$$

Since γ becomes temperature-dependent we conclude that energy ε_* now also depends on T:

$$\varepsilon_* = \hbar \Omega \sqrt{\gamma'} \propto T \sqrt{H}. \tag{81}$$

Low-field MR is still given by Eq. (59), where one should substitute expression (81) for ε_*. It is worth emphasizing that charged impurities yield temperature independent MR in contrasts to inverse temperature dependence of MR in the case of short range potential. The latter fact would allow one to distinguish these two scattering mechanisms in experiments.

VI. CONCLUSIONS

To conclude we studied magnetotransport in graphene with the short-range disorder within SCBA. We found that magnetoresistance depends on three relevant parameters having dimensionality of the energy, μ, T and ε_*, the field dependence being fully absorbed by ε_* which is proportional to $\sqrt{H}$.

One of the main predictions of our model is the square-root field dependence of magnetoresistance in the limit of low H, both at very low and at very high temperatures. Such a dependence persists down to exponentially small fields, corresponding to $\varepsilon_* \sim \Delta e^{-\pi\gamma/2}$.

We separately analyzed the cases of low and high temperatures and identified four different transport regimes for $\mu \gg T$ and three regimes for $\mu \ll T$ (see Fig. 3). All these regimes can be realized provided that temperature lays within a certain interval. Let us now find the corresponding criteria.

For $\mu \gg T$ and not too small ε_*, MR is determined by energies close to the Fermi surface, $\varepsilon \approx \mu$. Above we assumed that Shubnikov de Haas oscillations are suppressed by energy averaging within the temperature window, which implies that $T \gg \hbar\omega_c(\mu)$. Using Eqs. (3) and (10) this inequality can be rewritten as $\varepsilon_* \ll \sqrt{\gamma T \mu}$. While identifying regimes shown at the upper picture in the Fig. 3 we implicitly assumed that $\sqrt{\gamma T \mu}$ is larger than μ, or, equivalently, $T > \mu/\gamma$. When T becomes smaller than $T > \mu/\gamma$ the high-field square-root asymptotic of MR is not realized because of arising of Shubnikov de Haas oscillations at $\varepsilon_* \sim \sqrt{\gamma T \mu} \ll \mu$. However, the low-field square-root asymptotic is determined by energies $\varepsilon \sim \varepsilon_*$ and remains valid even at low temperature, because Eq. (12) is always satisfied for $T \ll \mu$ and $\varepsilon_* < \varepsilon_2$.

In the opposite limiting case, $T \gg \mu$, the main contribution to MR comes from $\varepsilon \approx \varepsilon_*$. Rewriting Eq. (12) as $\varepsilon_* \ll \gamma T$, we find that three regimes shown in Fig. 3 are realized provided that $\gamma T \gg T^2/\mu$, or, equivalently, $T \ll \gamma\mu$. At higher temperatures, $T \gg \gamma\mu$, MR is given by $C_3\varepsilon_*/2T$ for $\varepsilon_* \ll T$ and $C_4(\varepsilon_*/T)^3$ in the interval $T \ll \varepsilon_* \ll \gamma T$. The Shubnikov de Haas oscillations appear at $\varepsilon_* \gg \gamma T$.

We also predict a non-trivial behavior of the Hall coefficient on H in the vicinity of the Dirac point. With increasing the field, R decreases, reaches a minimum and then starts to grow again. Further, we analyzed dependence of R on electron concentration and found that this dependence is non-monotonic both for law and strong fields.

Importantly, the main prediction of our theory, the square root dependence of MR in the limit of weak fields, is also valid for the case of charged impurity potential. It is worth finally noting that our theory is applicable for any other 2D electron system with the linear energy spectrum such as topological insulators.[27,28]

Note added: After this work was completed the experimental evidence of square-root MR in monolayer graphene was reported.[29]

VII. ACKNOWLEDGEMENTS

We thank N.S. Averkiev, A.A. Greshnov, M.O. Nestoklon, M. Titov, and Yu. Vasilyev for fruitful discussions. The work was supported by DFG CFN, BMBF, DFG SPP “Graphene”, RFBR, RF President Grant ”Leading Scientific Schools” NSh-5442.2012.2, and by programs of the RAS,.

---

[1] T. Ando, Rev. Mod. Phys. **54**, 437 (1982).
[2] S. D. Sarma, S. Adam, E. H. Hwang, E. Rossi, Rev. Mod. Phys. **83**, 407 (2011).
[3] T. Ando and Y. Uemura, Journ. of the Phys. Soc. of Japan **36**, 956 (1974).
[4] T. Ando, Journ. of the Phys. Soc. of Japan **36**, 1521 (1974).
[5] T. Ando, Journ. of the Phys. Soc. of Japan **37**, 622 (1974).
[6] T. Ando, Journ. of the Phys. Soc. of Japan **37**, 1233 (1974).
[7] N. H. Shon and T. Ando, Journ. of the Phys. Soc. of Japan **67**, 2421 (1998).
[8] Y. Zheng and T. Ando, Phys. Rev. B **65**, 245420 (2002).
[9] V. P. Gusynin and S. G. Sharapov, Phys. Rev. B **71**, 125124 (2005); V. P. Gusynin and S. G. Sharapov, Phys. Rev. B **73**, 245411 (2006).
[10] N. M. R. Peres, F. Guinea, and A. H. Castro Neto, Phys. Rev. B **73**, 125411 (2006).
[11] B. Dora and P. Thalmeier, Phys. Rev. B **76**, 035402 (2007).
[12] P. M. Ostrovsky, I. V. Gornyi, and A. D. Mirlin, Phys. Rev. B **77**, 195430 (2008).
[13] M. Müller, L. Fritz, and S. Sachdev, Phys. Rev. B **78**, 115406 (2008).
[14] J. Jobst, D. Waldmann, I. V. Gornyi, A. D. Mirlin, and H. B. Weber, Phys. Rev. Lett. **108**, 106601 (2012)
[15] A.H. Castro Neto, F. Guinea, N.M.R. Peres, K.S. Novoselov, and A.K. Geim, Rev. Mod. Phys. **81**, 109 (2009)
[16] T. Ando and T. Nakanishi, Journ. of the Phys. Soc. of Japan **67**, 1704 (1998).
[17] P. M. Ostrovsky, I. V. Gornyi, and A. D. Mirlin, Phys. Rev. B **74**, 235443 (2006).
[18] I. A. Dmitriev, A. D. Mirlin, D. G. Polyakov, and M. A. Zudov, arXiv: cond-mat1111.2176v2 (2011).
[19] T. Ando, Y. Matsumoto, and Y. Uemura, Journ. of the Phys. Soc. of Japan **39**, 279 (1975).
[20] P. Středa, J. Phys. C, **15**, L717 (1982).
[21] M. G. Vavilov and I. L. Aleiner, Phys. Rev. B **69**, 035303 (2004).
[22] Within the SCBA, the transverse conductivity including

both $\sigma^{I}_{xy}(\varepsilon)$ and $\sigma^{II}_{xy}(\varepsilon)$ can be written as follows[19]

$$\sigma_{xy}(\varepsilon) = \frac{ecn(\varepsilon, H)}{H} - \frac{\sigma_{xx}(\varepsilon) z(\varepsilon)}{\omega_c(\varepsilon)\tau_{tr}(\varepsilon)}.$$

This is the classical relation between $\sigma_{xx}(\varepsilon)$ and $\sigma_{xy}(\varepsilon)$ where the τ_{tr} is replaced with τ_{tr}/z. Subtracting $\sigma^{I}_{xy}(\varepsilon)$ [given by Eq. (36)] from this relation, one finds a convenient representation for thermodynamical contribution to the Hall conductivity

$$\sigma^{II}_{xy}(\varepsilon) = \frac{e^2 N}{2\pi\hbar^3\Omega^2}\left[\int_0^{\varepsilon} z(\varepsilon')|\varepsilon'|d\varepsilon' - \frac{|\varepsilon|\varepsilon z(\varepsilon)}{2}\right].$$

Averaging the latter equation over energy within the interval $\delta\varepsilon$ one finds that the thermodynamical contribution can be neglected.

[23] In the energy range $\varepsilon \gg \varepsilon_*$ corresponding to overlapping Landau levels, $\sigma^{II}_{xy}(\varepsilon)$ is exponentially small and besides that is an oscillatory function of energy, whereas the exponentially small correction to $\sigma^{I}_{xy}(\varepsilon)$ contains a non-oscillatory term. Therefore, energy-averaged contribution to the transverse conductivity, $\bar{\sigma}^{II}_{xy}(\varepsilon)$, is smaller than the exponential correction to $\bar{\sigma}^{I}_{xy}(\varepsilon)$.

[24] M. Schütt, P.M. Ostrovsky, I.V. Gornyi, and A.D. Mirlin, Phys. Rev. B **83**, 155441 (2011).

[25] B.N. Narozhny, M. Titov, I.V. Gornyi, and P.M. Ostrovsky, Phys. Rev. B **85**, 195421 (2012).

[26] One can show that crossover from Eq. (73) to Eq. (66) happens in the interval of concentration corresponding to $T < \mu < T\ln[\ln(T/\varepsilon_*)]$.

[27] M. Z. Hasan, C. L. Kane, Rev. Mod. Phys. **82**, 3045 (2010).

[28] X.-L. Qi and S.-C. Zhang, Rev. Mod. Phys. **83**, 1057 (2011).

[29] G.Yu. Vasilyeva et al, Pis'ma v ZhETP, **96**, 519 (2012).